Atomically resolved study of the morphology change of InAs/GaAs quantum dot layers induced by rapid thermal annealing

Atomically resolved study of the morphology change of InAs/GaAs quantum dot layers induced by rapid thermal annealing

J. G. Keizer,[1] A. B. Henriques,[2] A. D. B. Maia,[2] A. A. Quivy,[2] and P. M. Koenraad[1]
[1]*Department of Applied Physics, Eindhoven University of Technology, P.O. Box 513, NL-5600 MB Eindhoven, The Netherlands*
[2]*Instituto de Fisica, Universidade de São Paulo, C.P. 66318, 05315-970 São Paulo, Brazil*

(Received 9 August 2012; accepted 26 November 2012; published online 12 December 2012)

The optoelectronic properties of InAs/GaAs quantum dots can be tuned by rapid thermal annealing. In this study, the morphology change of InAs/GaAs quantum dots layers induced by rapid thermal annealing was investigated at the atomic-scale by cross-sectional scanning tunneling microscopy. Finite elements calculations that model the outward relaxation of the cleaved surface were used to determine the indium composition profile of the wetting layer and the quantum dots *prior* and *post* rapid thermal annealing. The results show that the wetting layer is broadened upon annealing. This broadening could be modeled by assuming a random walk of indium atoms. Furthermore, we show that the stronger strain gradient at the location of the quantum dots enhances the intermixing. Photoluminescence measurements show a blueshift and narrowing of the photoluminescence peak. Temperature dependent photoluminescence measurements show a lower activation energy for the annealed sample. These results are in agreement with the observed change in morphology. [http://dx.doi.org/10.1063/1.4770371]

Self-assembled quantum dots (QDs) fabricated by heteroepitaxial growth have attracted much attention in the last decade. The zero-dimensional nature of these nanostructures can be exploited in optoelectronic devices, such as QD lasers,[1,2] single-photon emitters,[3] single-electron transistors,[4] and spin-manipulation.[5,6] Control over the emission wavelength is important in such devices and academic studies. The two most widely exploited parameters to tune the emission wavelength are the QD height and the composition. Decreasing the height raises the energy levels of the QD and increases the interband transition energy, while intermixing of QD and host material lowers the potential barrier. Both processes lead to a blueshift of the emission wavelength. Various techniques exist to control the height, e.g., double capping,[7] indium-flush,[8] Sb-capping,[9] while the composition can readily be tuned by supplying the appropriate material during the epitaxial growth of the QD layers. However, both techniques require delicate tuning of the growth parameters. In this respect, the technique of *post* growth rapid thermal annealing (RTA) is much simpler. It is generally accepted that RTA leads to intermixing in InAs/GaAs QDs[10–18] and that the technique can blueshift the emission wavelength of the QDs over a relatively large energy range (up to 350 meV).

In this paper, we report on the effect of RTA on InAs/GaAs QD layers. Cross-sectional scanning tunneling microscopy (XSTM) was used to study the morphology of QD layers in *as grown* and *annealed* samples with atomic resolution. Finite element (FE) calculations that model the outward surface relaxation of the cleaved sample are used in conjunction with XSTM results to precisely determine the composition of the QD layers. A simple diffusion model that describes the change in morphology is proposed. Low temperature and temperature dependent photoluminescence (PL) measurements were performed on both samples.

The sample consists of InAs/GaAs QD layers grown by MBE on a *n*-doped (001)-oriented GaAs substrate. First, a 200 nm GaAs buffer layer was grown at 570 °C, followed by 35 nm GaAs grown at 510 °C, the nominal growth temperature. Next, a sequence that consists of a Si δ-doping layer, 15 nm GaAs, 2.4 monolayer (ML) InAs, 15 nm GaAs, a Si δ-doping layer, and 20 nm GaAs was repeated ten times. The δ-doping layers were inserted to obtain an average occupation of one electron per QD,[19] but are of no further interest in the current study. Finally, the sample was capped with 45 nm GaAs.

The PL-measurements were done in a variable temperature optical cryostat. The QD layers were excited by the 532 nm line of a frequency-doubled Nd:YAG laser. Typical excitation powers were $\approx 4\,\mathrm{W\,cm^{-2}}$.

The RTA was done using an AG Associates HeatPulse 410 system. The sample chamber was purged with room temperature N_2 gas. The sample was heated to 950 °C at a rate of $80\,^{\circ}\mathrm{C\,s^{-1}}$ and held at 950 °C for 30 s, after which it

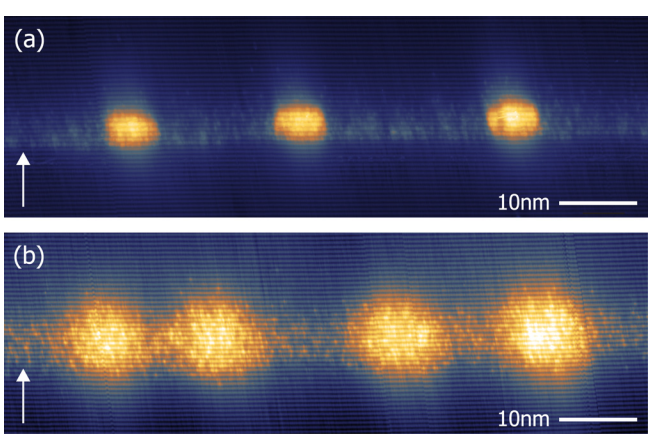

FIG. 1. Topographic XSTM images of two typical stretches of the QD layer in (a) the *as grown* and (b) the *annealed* sample. The arrows indicate the growth direction.

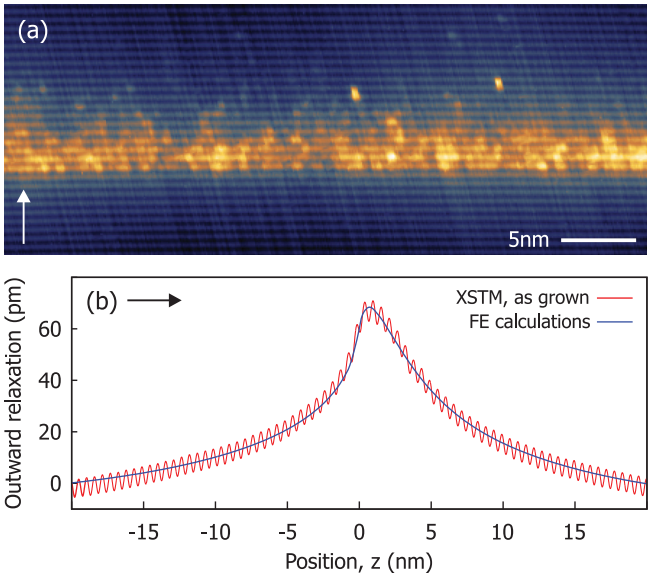

FIG. 2. (a) XSTM close-up of a typical part of the WL in the *as grown* sample. (b) Outward surface relaxation, averaged over 50 nm, as measured with XSTM (red line) and the result of the FE calculations (blue line). The arrows indicate the growth direction.

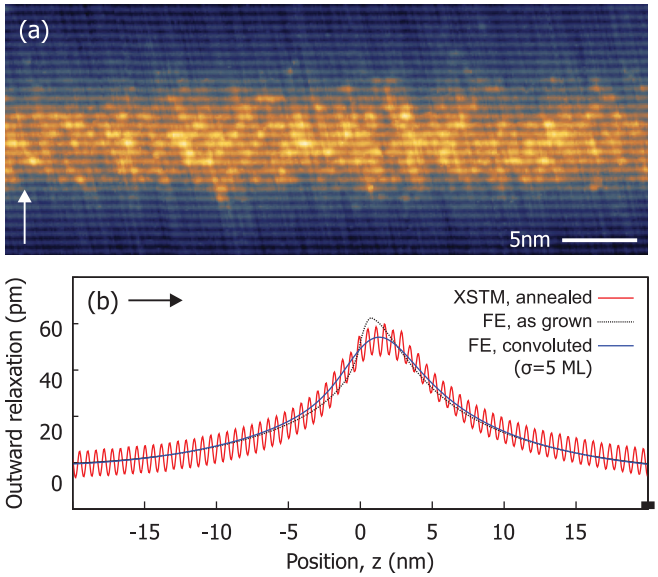

FIG. 3. (a) XSTM close-up of a typical part of the WL in the *annealed* sample. (b) Outward surface relaxation, averaged over 50 nm, as measured with XSTM (red line), the result of the FE calculations for the *as grown* indium profile (dotted black line) and the convoluted indium profile (blue line). The arrows indicate the growth direction.

was rapidly cooled to room temperature. The sample surface was completely covered with a GaAs substrate in order to avoid sublimation induced arsenic losses.

The XSTM measurements were performed at room temperature under UHV conditions ($p < 5 \times 10^{-11}$ mbar) on *in situ* cleaved (110)-surfaces. All measurements were done at high negative bias voltage and low tunnel current ($V \approx -3$ V, $I \approx 40$ pA). At these tunnel conditions and with the color scale used, InAs (GaAs) rich regions appear bright (dark). Upon cleavage of a strained material system, the surface relaxes. This minute displacement of the surface can be recorded in careful XSTM measurements. In conjunction with FE calculations, this information can be used to deduce the local composition of the material system.[20–22] In the current paper, the outward surface relaxation induced by the wetting layers (WLs) and QDs is modeled by 2D and 3D FE calculations, respectively.

Figure 1 shows topographic XSTM images of two typical stretches of the QD layer in the *as grown* and the *annealed* sample. In both cases, the WL and QDs can clearly be distinguished. The difference between the two cases is striking: the dimensions of both the WL and the QDs appear much larger in the *annealed* sample. Evidently, the RTA has a dramatic influence on the morphology of the QD layers. This will now be investigated in more detail, first for the WLs followed by the QDs.

A close-up of the WL in the *as grown* sample is shown in Figure 2(a). Individual indium atoms as well as the atomic planes can be distinguished. The WL is found to start abruptly (within one bilayer), followed by a decay of the indium concentration in the direction of growth. From previous work, it is known that the decay can be described by the phenomenological model proposed by Muraki *et al.*[23]

$$x(n) = \begin{cases} 0, & n < 1 \\ x_0(1 - R^n), & 1 \le n \le N \\ x_0(1 - R^N)R^{n-N}, & n > N \end{cases},$$

where $x_0 = 1$ is the nominal indium concentration of the WL, n the ML index, N the total amount of deposited indium, and R the indium segregation coefficient. The above model is used as input in the FE modeling of the outward surface relaxation induced by the WL. By adjusting the parameters R and N until the calculated outward surface relaxation (blue line, Figure 2(b)) matches the outward surface relaxation as measured by XSTM (red line, Figure 2(b)), the decay of the indium concentration can be determined. We find $R = 0.88 \pm 0.01$ and $N = 1.45 \pm 0.05$, which are typical values for InAs/GaAs WLs.[20,24]

In Figure 3(a)), a typical stretch of the *annealed* WL is shown. In striking contrast to the *as grown* sample, in the *annealed* sample the WL is much thicker, the lower GaAs/WL interface diffuse, and the indium concentration along the growth direction decreases more slowly. In Figure 3(b), the experimentally observed outward surface relaxation of the *annealed* WL (red line) is compared with the calculated outward surface relaxation of the *as grown* WL (dotted black line). We find that the two do not match, which is not surprising given the observed redistribution of indium. To model the redistribution, we convolute the indium concentration profile with the 1D normal distribution

$$f(z, \sigma_z) = \frac{1}{\sigma_z\sqrt{2\pi}} \exp^{-\frac{1}{2}\left(\frac{z}{\sigma_z}\right)^2},$$

with z the position coordinate along the growth direction and σ_z the standard deviation, the only parameter used for fitting. Physically, a convolution with the normal distribution means that the indium atoms are subjected to a random walk during annealing. Note that, this is a first order model in which the extension of the random walk, σ, is taken to be independent of the indium concentration. The original (red line) and a convoluted indium concentration profile (blue line) are shown in Figure 4. The convoluted profiles were used as

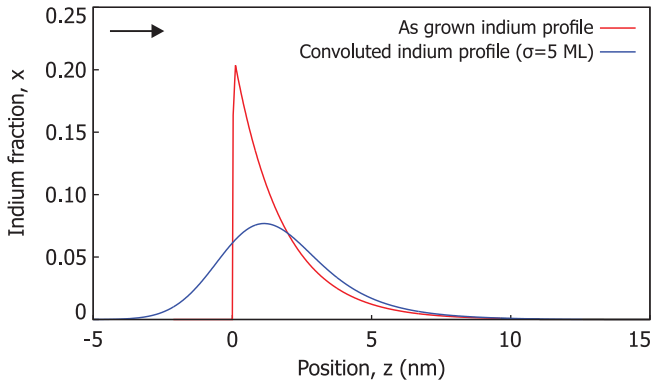

FIG. 4. Indium composition profile that yields the best fit with the outward surface relaxation of the *as grown* WL (red line), and the result of the convolution of this profile with a normal function (blue line). The arrow indicates the growth direction.

input for the FE calculations. An excellent fit of the calculated with the experimentally observed outward surface relaxation was found for $\sigma = 5 \pm 1$ ML, see Figure 3(b).

We now turn our attention to the QDs. Approximately 50 QDs were observed in both samples. The average QD height in the *annealed* sample was found to be 4 ± 0.5 nm, with a width in the 4–10 nm range. Again, FE calculations are used in conjunction with the observed outward surface relaxation to determine the composition profile. The QDs were modeled, analog to Ref. 22, as truncated pyramids with a linear increasing (bottom to top) indium fraction flanked by the WL as determined above. Due to the arbitrary position of the cleavage plane in XSTM, we have no *a priori* way of knowing how a particular QD is cleaved. This problem can be circumvented by selecting one of the widest QDs in the ensemble for our analysis. In this way, one can be reasonably sure that the selected QD is cleaved through its center. In Figure 5(a/c), one of the widest QD from each sample is shown. As with the WLs, a clear difference between the two is observed: the *as grown* QD is much more localized and appears much brighter. Note that the range of the color scale is the same in both images. The enhanced brightness of the *as grown* QD is the result of a larger outward surface relaxation due to a higher indium concentration.

The best match with the observed outward surface relaxation of the *as grown* QD was found for $x = 0.55$ (bottom) and $x = 0.85$ (top), see Figure 5(b/e). The fit could be slightly improved by adding an exponential indium decay in the growth direction on top of the QD ($x_0 = 0.09$, same decay rate as the WL). In our previous work on InAs QDs, this feature was also found.[24]

The *annealed* QDs are modeled by convoluting the *as grown* QDs with a 3D normal distribution ($\sigma_x = \sigma_y = \sigma_z$). The best fit of the FE calculations to the experimentally observed outward surface relaxation was found for $\sigma = 10 \pm 1$ ML, see Figure 5(d/e). Note that, the maximum indium fraction in the QD has now dropped to $x = 0.36$. The extension of the random walk, σ, is significantly larger than in case of the WL. For quantum wells, it has been shown that the diffusion length of the constituent atoms is not fixed but instead is a function of the local gradient in strain.[25] The same was speculated in previous investigations of RTA on InAs/GaAs QDs.[10–12] These studies were based on PL-measurements and simulations, and as such, the results

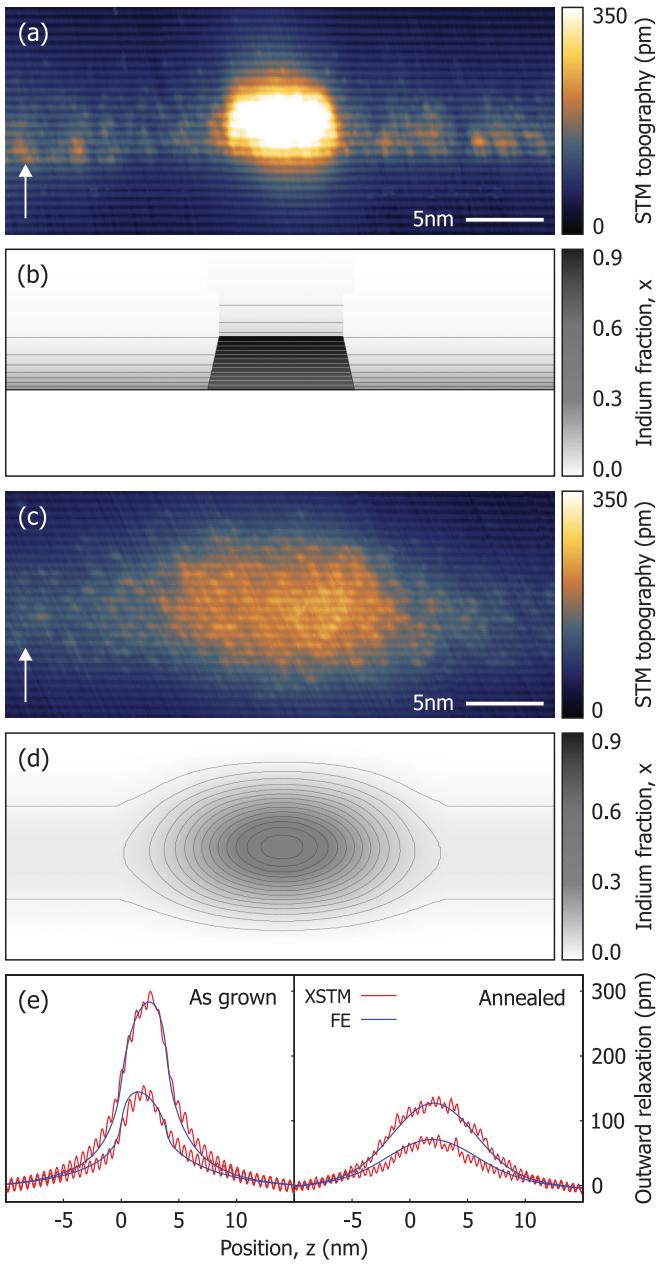

FIG. 5. Typical QDs as observed with XSTM in the (a) *as grown* and (b) the *annealed* sample. The range of the color scale is the same for both cases. The arrows indicate the growth direction. (b) and (d) Corresponding QD models that yield the best fit with the observed outward surface relaxation. The contour lines are every 2.5%, ranging from 0% to 90%. (e) Outward surface relaxation through the center and 5 nm off-center of the *as grown* and the *annealed* QD.

could not directly be linked to the morphology of the QD layer. Here, the juxtaposition of XSTM and FE calculations unambiguously shows the change in morphology of the QD layer and the difference in strength of intermixing in the WL vs. QDs. The intermixing is due to two contributions. The first contribution is thermal activated random diffusion of atoms, which is independent of the indium concentration. The second contribution is non-random drift of atoms due to local strain gradients. At the location of the QDs, the strain gradients are larger compared to the WL, resulting in a local increase of intermixing. Unfortunately, it is not possible to separate these two contributions in the current work. Both contributions are (nearly) symmetrical and on the same length-scale. As a result, the solution of the calculated

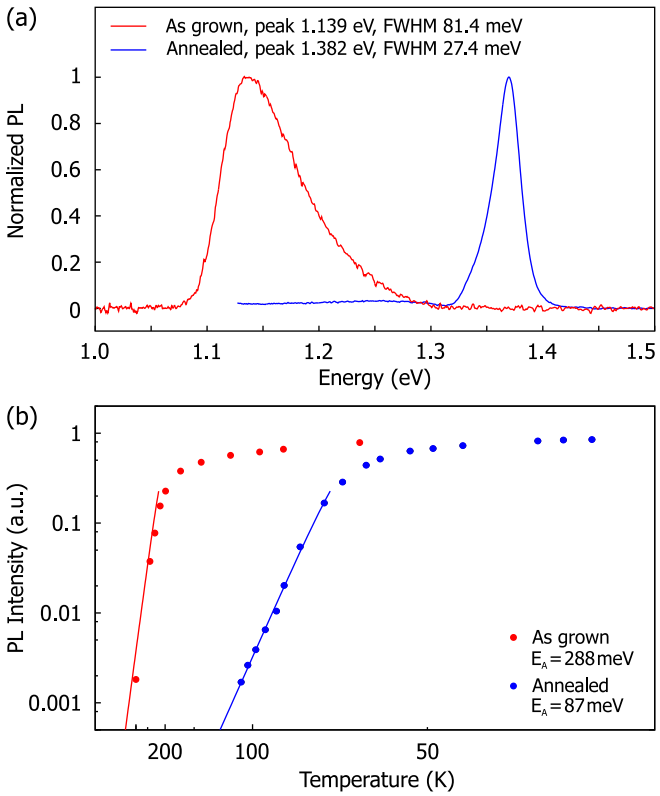

FIG. 6. (a) Normalized PL-spectra (6 K) taken on the *as grown* (red line) and the *annealed* (blue line) sample. (b) Temperature dependence of the peak PL-intensity for the *as grown* (red dots) and the *annealed* (blue dots) sample.

outward surface relaxation is not unique. Nevertheless, the current results show that the diffusion at the QD region can be considered as isotropic, excluding previous suggestions that lateral or vertical diffusion is favored.[12,17]

As shown above, RTA causes intermixing between the QDs and the host material. This has consequences for the emission properties. Figure 6(a), shows PL-spectra taken on both samples. The peak PL-position is shifted towards higher energy after RTA. As the XSTM results show, indium diffuses out of the QDs and is replaced by gallium. This results in an increase of the QD band gap and hence a blueshift. In addition, the intermixing of QD and host material increases the size of the QDs, and as a consequence, the ratio between size fluctuations and the average QD size decreases. This causes the QD band gaps in the ensemble to become much more similar to one another, and consequently, the full width half maximum (FWHM) of the inhomogeneously broadened PL-line drops.

Temperature dependent PL-measurements were performed on both samples, see Figure 6(b). The quenching of the PL-intensity, I, when the temperature, T, is increased is well described by an exponential dependence, $I \sim e^{E_A/k_B T}$, shown by the straight lines in Figure 6(b). The activation energy, E_A, is lower after RTA. With increasing temperature, it is known that photo-excited carriers in the QD are thermally excited into the WL and thereby quench the PL-intensity.[26] This is explained by the blue shift of the QD PL-emission after annealing, which brings the QD band gap in the annealed sample much closer to the band gap of the WL, hence the activation energy decreases.

To summarize, we have investigated the morphology change of InAs/GaAs QDs induced by RTA on the atomic scale by means of XSTM. We show that the WL and the QDs are subjected to direction independent indium diffusion on the nanometer scale. The diffusion is found to be significantly larger at the position of the QDs where the strain is locally higher. Low temperature PL-measurements show a blueshift and narrowing of the PL-peak. Temperature dependent PL-measurements show a decrease in the activation energy for the *annealed* sample. Both results are in agreement with the observed change in morphology.

A.B.H. acknowledges financial support provided by CNPq (Grants 304685/2010-0 and 475296/2009-5), by FAPESP (Grant 2010/10452-8), and by LNLS/LMF-Brazilian Synchrotron Light Laboratory.

[1]S. Fafard, K. Hinzer, S. Raymond, M. Dion, J. McCaffrey, Y. Feng, and S. Charbonneau, Science **274**, 1350 (1996).
[2]F. Heinrichsdorff, M.-H. Mao, N. Kirstaedter, A. Krost, D. Bimberg, A. O. Kosogov, and P. Werner, Appl. Phys. Lett. **71**, 22 (1997).
[3]Z. Yuan, B. E. Kardynal, R. M. Stevenson, A. J. Shields, C. J. Lobo, K. Cooper, N. S. Beattie, D. A. Ritchie, and M. Pepper, Sciences (N.Y.) **295**, 102 (2002).
[4]K. Yano, T. Ishii, T. Hashimoto, T. Kobayashi, F. Murai, and K. Seki, IEEE Trans. Electron Devices **41**, 1628 (1994).
[5]D. Loss and D. P. DiVincenzo, Phys. Rev. A **57**, 120 (1998).
[6]S. Chakrabarti, M. A. Holub, P. Bhattacharya, T. D. Mishima, M. B. Santos, M. B. Johnson, and D. A. Blom, Nano Lett. **5**, 209 (2005).
[7]C. Paranthoen, N. Bertru, O. Dehaese, A. Le Corre, S. Loualiche, B. Lambert, and G. Patriarche, Appl. Phys. Lett. **78**, 1751 (2001).
[8]J. G. Keizer, E. C. Clark, M. Bichler, G. Abstreiter, J. J. Finley, and P. M. Koenraad, Nanotechnology **21**, 215705 (2010).
[9]W. Lu, M. Bozkurt, J. G. Keizer, T. Rohel, H. Folliot, N. Bertru, and P. M. Koenraad, Nanotechnology **22**, 055703 (2011).
[10]F. Heinrichsdorff, M. Grundmann, O. Stier, A. Krost, and D. Bimberg, J. Cryst. Growth **195**, 540 (1998).
[11]S. Fafard and C. N. Allen, Appl. Phys. Lett. **75**, 2374 (1999).
[12]A. Babiński, J. Jasiński, R. Bozek, A. Szepielow, and J. M. Baranowski, Appl. Phys. Lett. **79**, 2576 (2001).
[13]Q. D. Zhuang, J. M. Li, X. X. Wang, Y. P. Zeng, Y. T. Wang, B. Q. Wang, L. Pan, J. Wu, M. Y. Kong, and L. Y. Lin, J. Cryst. Growth **208**, 791 (2000).
[14]T. M. Hsu, Y. S. Lan, W.-H. Chang, N. T. Yeh, and J.-I. Chyi, Appl. Phys. Lett. **76**, 691 (2000).
[15]Z. Zhang, P. Jin, C. Li, X. Ye, X. Meng, B. Xu, F. Liu, and Z. Wang, J. Cryst. Growth **253**, 59 (2003).
[16]G. Shi, P. Jin, B. Xu, C. Li, C. Cui, Y. Wang, X. Ye, J. Wu, and Z. Wang, J. Cryst. Growth **269**, 181 (2004).
[17]T. Yang, J. Tatebayashi, K. Aoki, M. Nishioka, and Y. Arakawa, Appl. Phys. Lett. **90**, 111912 (2007).
[18]Q. Cuao, S. F. Yoon, C. Y. Liu, and C. Z. Tong, J. Appl. Phys. **104**, 033522 (2008).
[19]A. Henriques, A. Schwan, S. Varwig, A. Maia, A. Quivy, D. Yakovlev, and M. Bayer, Phys. Rev. B **86**, 115333 (2012).
[20]P. Offermans, P. M. Koenraad, R. Notzel, J. H. Wolter, and K. Pierz, Appl. Phys. Lett. **87**, 111903 (2005).
[21]J. H. Davies, D. M. Bruls, J. W. A. M. Vugs, and P. M. Koenraad, J. Appl. Phys. **91**, 4171 (2002).
[22]D. M. Bruls, J. W. A. M. Vugs, P. M. Koenraad, H. W. M. Salemink, J. H. Wolter, M. Hopkinson, M. S. Skolnick, F. Long, and S. P. A. Gill, Appl. Phys. Lett. **81**, 1708 (2002).
[23]K. Muraki, S. Fukatsu, Y. Shiraki, and R. Ito, Appl. Phys. Lett. **61**, 557 (1992).
[24]A. D. Giddings, J. G. Keizer, M. Hara, G. J. Hamhuis, H. Yuasa, H. Fukuzawa, and P. M. Koenraad, Phys. Rev. B **83**, 205308 (2011).
[25]S.-W. Ryu, I. Kim, B.-D. Choe, and W. G. Jeong, Appl. Phys. Lett. **67**, 1417 (1995).
[26]S. Fafard, S. Raymond, G. Wang, R. Leon, D. Leonard, S. Charbonneau, J. L. Merz, P. M. Petroff, and J. E. Bowers, Surf. Sci. **361–362**, 778 (1996).